

# TacCompress: A Benchmark for Multi-Point Tactile Data Compression in Dexterous Manipulation

Yang Li<sup>1\*</sup>, Yan Zhao<sup>2\*</sup>, Zhengxue Cheng<sup>1,2</sup> and Hengdi Zhang<sup>1</sup>

**Abstract**—Though robotic dexterous manipulation has progressed substantially recently, challenges like in-hand occlusion still necessitate fine-grained tactile perception, leading to the integration of more tactile sensors into robotic hands. Consequently, the increased data volume imposes substantial bandwidth pressure on signal transmission from the hand’s controller. However, the acquisition and compression of multi-point tactile signals based on the dexterous hands’ physical structures have not been thoroughly explored. In this paper, our contributions are twofold. First, we introduce a Multi-Point Tactile Dataset for Dexterous Hand Grasping (Dex-MPTD). This dataset captures tactile signals from multiple contact sensors across various objects and grasping poses, offering a comprehensive benchmark for advancing dexterous robotic manipulation research. Second, we investigate both lossless and lossy compression on Dex-MPTD by converting tactile data into images and applying six lossless and five lossy image codecs for efficient compression. Experimental results demonstrate that tactile data can be losslessly compressed to as low as 0.0364 bits per sub-sample (bps), achieving approximately 200× compression ratio compared to the raw tactile data. Efficient lossy compressors like HM and VTM can achieve about 1000× data reductions while preserving acceptable data fidelity. The exploration of lossy compression also reveals that screen-content-targeted coding tools outperform general-purpose codecs in compressing tactile data.

## I. INTRODUCTION

Tactile perception is fundamental to human sensing, enabling the recognition of object properties such as shape, texture, and temperature, while providing essential feedback for precise manipulations [1]. Recently, robotic dexterous hands have been designed to offer more contact points and flexible fingertip configurations, facilitating complex grasping poses and finer manipulations for objects of varying shapes and sizes. However, this advancement has also led to a surge in tactile data volume. Specifically, modern robotic hands are equipped with more than ten tactile sensors, and improvements in measurement accuracy and spatial resolution have resulted in an exponential data growth [2], a challenge that has been largely overlooked in the past. As shown in Fig. 1, tactile data compression not only reduces the bandwidth consumption but also enhances system response speed and efficiency in real-time processing tasks [3].

Various approaches have been proposed to investigate the compression of tactile data [4], [5], [6], [7], [8], [9]. Traditional signal processing techniques, such as dimensionality

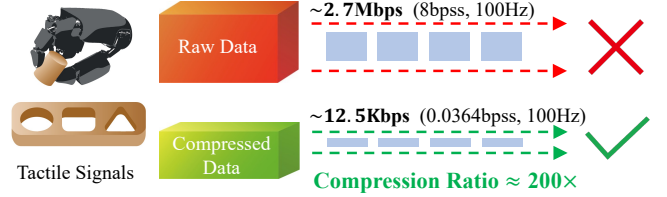


Fig. 1: For a dexterous hand, at a frequency of 100Hz, the raw tactile data occupies a bandwidth of about 2.7 Mbits per second ( $100 \text{ Hz} \times 1140 \text{ units} \times 3 \text{ axis} \times 8 \text{ bps}$ ), while after data format conversion and applying lossless compression we proposed, the required bandwidth drops to 12.5 Kbits per second ( $100 \text{ Hz} \times 1140 \text{ units} \times 3 \text{ axis} \times 0.0364 \text{ bps}$ ), achieving more than 200× data volume reductions.

reduction and transformation-based approaches, help reduce data redundancy but often struggle to fully preserve the complex features of tactile information [10]. Besides, with the rapid development of artificial intelligence in recent years, neural network-based compression [11], [12] has emerged as a new research focus, especially for high-dimensional data, such as speech, image, and tactile, etc. Compared to traditional compression methods [13], [14], [15], [16], [17], neural network-based compression techniques can automatically learn the low-dimensional representation of data, thus realizing efficient, lossless or near-lossless compression [18].

Most existing tactile compression methods are designed for single-sensor processing and do not fully account for the role of the dexterous hand’s physical structure in tactile perception [19], [20], [21]. In fact, traditional studies on tactile recognition of dexterous hands are usually limited to fingertip-based sensing, which is often insufficient for multi-task grasping and manipulation [22]. Many manipulation tasks require multiple points of contact between the robot and the object, similar to how humans perceive objects through multi-finger interactions. With advancements of tactile data acquisition, emerging technologies like artificial skin and finger-like tactile sensors have expanded the potential for multi-point tactile sensing [23]. Hence, there remains urgent needs to develop and optimize compression algorithms for multi-point tactile datasets.

Our contributions can be summarized as:

- We introduce a Multi-Point Tactile Dataset for Dexterous Hand Grasping (Dex-MPTD), which captures tactile signals from multiple contact points across the dexterous hand. By incorporating the spatial distribution of tactile feedback influenced by the hand’s structure and

\* Both authors contributed equally to this work.

[.]<sup>1</sup> are with PaXini Tech., Shenzhen, China. [.]<sup>2</sup> are with Institute of Image Communication and Network Engineering, Shanghai Jiao Tong University, China. Emails: {liyang@paxini.com, zhaoyanzhy@sjtu.edu.cn, zxcheng@sjtu.edu.cn, zhanghd@paxini.com, Corresponding Author: Zhengxue Cheng. }

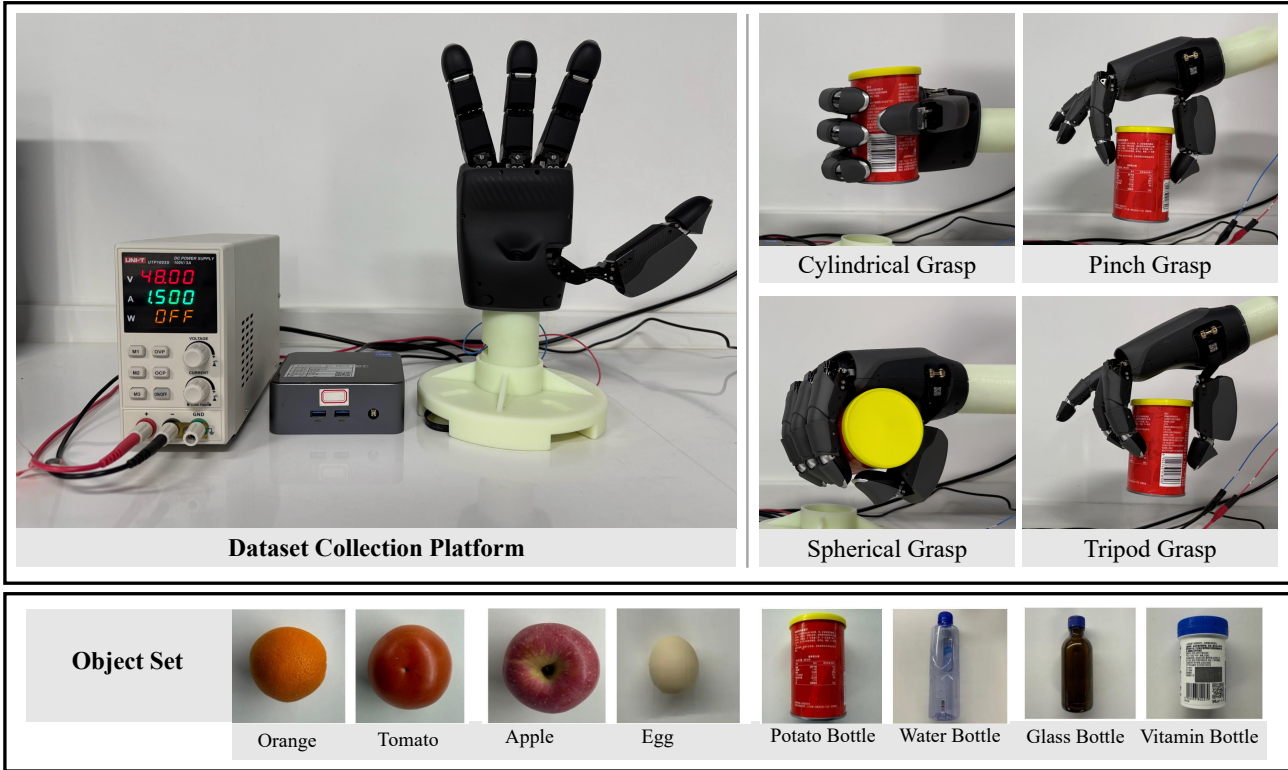


Fig. 2: The dataset collection platform we used (drawn in upper-left part), and four different grasping modes (upper-right part). Various eight types of objects are included in our experiment (bottom).

grasping poses, this dataset provides a comprehensive benchmark designed to advance research in dexterous robotic manipulation.

- We convert the collected tactile signals to images and conduct a comprehensive data compression evaluation. We adopt six lossless and five lossy compressors, including both traditional codecs and modern neural codecs for a fair comparison.
- Experimental results show that lossless compression can reduce data volume to 0.0364 bpss (about 200× data reduction), significantly easing transmission and storage demands. Highly efficient lossy compression further achieves about 1000× data reduction while maintaining acceptable distortion levels. Applications in object classification task also demonstrates the effectiveness of our proposed compression method.

## II. RELATED WORK

### A. Tactile Dataset

Tactile datasets are essential for robotic tactile research, particularly in grasping, object recognition, and manipulation tasks. The STAG dataset [24] captures 135,000 frames of full-hand interactions with 26 objects, facilitating studies on hand-object spatial relationships. The VTG dataset [20] includes 18 objects with different textures, sizes, and hardness, recording 435 data points per object, including finger angles and 3D force data, to analyze tripod grasp mechanics. The Poselt dataset [25] features 1840 grasping data points

from 26 objects across 16 grasping postures, integrating RGB-D images, tactile data, force, and torque. The RBO Hand dataset [26] captures tactile signals from multi-finger grasping and supports visual-tactile fusion for manipulation research. The RBOI dataset [21] focuses on fingertip sensing and motion planning, detecting surface variations for object recognition and grasp success prediction.

Other datasets explore material properties and tactile interactions. The PFN-VT dataset [27] records tactile data from 25 materials using a Sawyer robotic end-effector with uSkin sensors to estimate surface roughness and smoothness. The tactile signature dataset [28], one of the largest open-access tactile datasets, captures hand tactile data from 22 subjects performing 21 daily activities. The 3D object dataset [29] integrates Kinect V2 and other sensors to support robotic grasping and object recognition research. The multimodal tactile dataset [30] combines pressure, gravity, angular velocity, and magnetic field data to enhance tactile texture classification through machine learning. The Baxter tactile dataset [31] collects feedback across multiple objects and grasping poses for robot perception studies. The Ego pressure dataset provides pressure intensity data for each contact point, aiding research on tactile contact and pressure interaction [32].

However, few open-source datasets focus on multi-degree-of-freedom dexterous hands, equipped with multi-point array-based tactile sensors. Thus in this paper, we introduce a tactile dataset based on a multi-degree-of-freedom dexterous hand to support diverse research and industry applications.

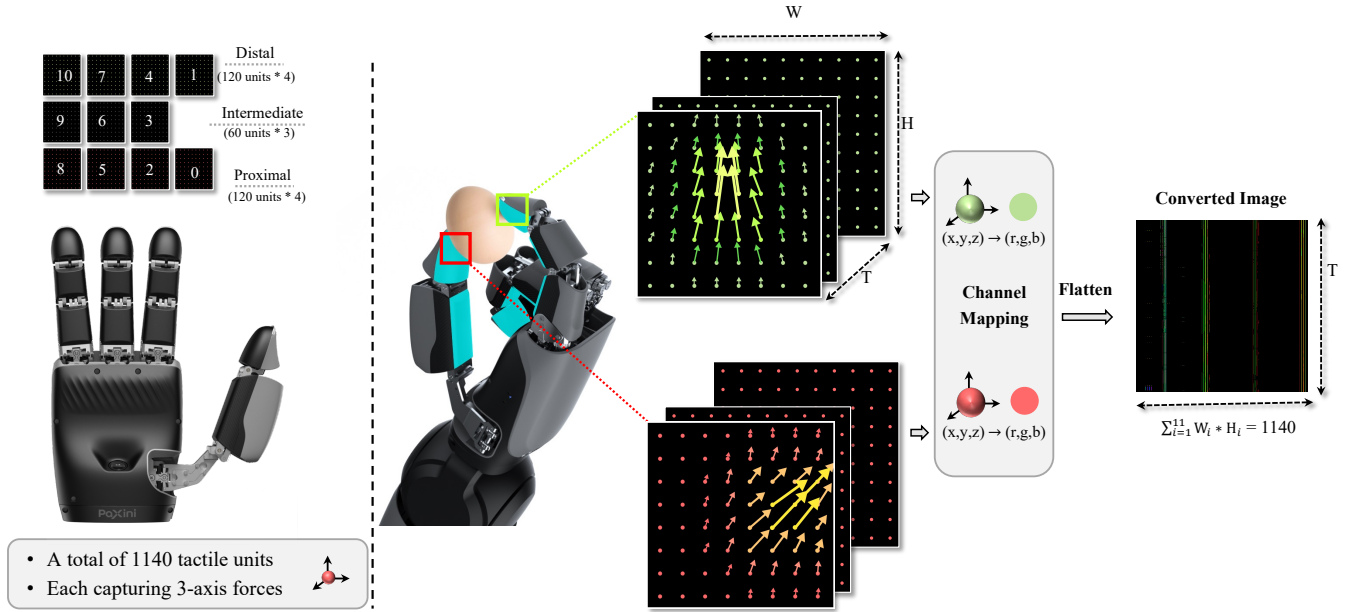


Fig. 3: The conversion method to transform force data into images, using a dexterous hand equipped with 11 sensors and 1140 tactile units, each capable of capturing 3-axis force measurements. The three-axis force data is mapped to RGB color components. These values are then raster-scanned to form the width of the images, while the sequential data along the timestep determines the height of the images.

### B. Tactile Compression Methods

As robot tactile sensors generate increasingly large and frequent data streams, tactile data transmission and storage become more challenging, especially given the bandwidth limitations of micro-control units (MCUs) in robotic hands. Uncompressed tactile data may exceed bandwidth constraints, degrading system performance and slowing response speed. Therefore, data compression is essential to reduce bandwidth load and conserve storage.

Recently, some studies on efficient tactile data compression have been proposed to enhance real-time interaction and reduce storage cost. For instance, the work [4] applies compressed sensing principles to tactile sensor arrays, leveraging signal sparsity to minimize data volume. E. Steinbach *et al.* [6] introduces a codec framework for low-latency and high-fidelity tactile data transmission. Shao *et al.* [5] demonstrates that mechanical waves generated by dynamic touch enable efficient tactile signal encoding. A. Slepyan *et al.* [7] suggests that wavelet transforms can effectively sparsity and compress tactile signals, reducing bandwidth requirements while maintaining perceptual integrity. The work [9] introduces a kinesthetic coding algorithm that leverages dead-zone coding and segmented linear prediction. Lu *et al.* [8] proposes a cross-modal tactile signal compression framework that leverages visual semantics and multi-head attention to optimize tactile encoding.

However, existing tactile compression methods focus primarily on single-sensor processing and overlook the role of dexterous hand structure in tactile perception. Therefore, we provide a data conversion strategy and leverage the efficient image coding methods for tactile signal compression, to

remove the spatial and temporal correlation better.

### III. DATASET COLLECTION

This section presents our data collection platform and the procedure for acquiring the Multi-Point Tactile Dataset (MPTD), as illustrated in Fig. 2.

#### A. Data Collection Platform

While numerous tactile datasets exist, most of them focus on single sensor for simple grasping or pinching tasks, with few open-source datasets based on multi-degree-of-freedom dexterous hands equipped with multiple tactile sensors. These existing datasets often fall short when it comes to complex tasks involving high-precision, multi-tasking, or multi-object manipulation, which limits their applications in advancing intelligent robots for multi-degree-of-freedom manipulation. Therefore, we present a tactile dataset built on a multi-degree-of-freedom dexterous hand *DexHI3* developed by PaXiniTech [33], as illustrated in Fig. 2. This dataset involves four different grasping poses, providing researchers with diverse experimental conditions.

As shown in Fig. 2, the data collection platform consists of PaXiniTech's dexterous hand, a 48-volt DC power supply, and a hand controller. The dexterous hand has four flexible fingers, each driven by a rotary motor, enabling actions like grasping, gripping, pinching, pressing, and finger opening and closing. This design mimics human hand gestures, allowing a more accurate presentation of complex tactile scenarios. By precisely controlling the four fingers, we can capture multi-point tactile data across various movement modes. As shown in Fig. 3, the dexterous hand has a total of

TABLE I: Lossless compression performance (bps) across objects and grasping poses. The uncompressed raw data by default has 8 bits per sub-sample, then compression ratio (CR) in the last row is calculated by  $8.0 / \text{bps}$ .

Settings		BPG	FLIF	JPEG-XL	WebP	GZIP	L3C
Object	Orange	0.0665	0.0491	0.0509	0.0396	0.0622	0.0616
	Tomato	0.0617	0.0441	0.0430	0.0345	0.0585	0.0575
	Apple	0.0756	0.0486	0.0528	0.0452	0.0706	0.0669
	Egg	0.0402	0.0290	0.0308	0.0236	0.0403	0.0434
	Potato Bottle	0.0650	0.0453	0.0438	0.0355	0.0583	0.0580
	Water Bottle	0.0570	0.0438	0.0405	0.0321	0.0567	0.0571
	Glass	0.0635	0.0448	0.0467	0.0411	0.0625	0.0613
	Vitamin Bottle	0.0662	0.0481	0.0459	0.0398	0.0621	0.0608
Grasp	Pinch	0.0567	0.0411	0.0407	0.0339	0.0537	0.0550
	Tripod	0.0570	0.0438	0.0409	0.0339	0.0552	0.0560
	Cylindrical	0.0730	0.0465	0.0517	0.0416	0.0655	0.0642
	Spherical	0.0601	0.0443	0.0439	0.0357	0.0600	0.0570
Average bps		<b>0.0619</b>	<b>0.0441</b>	<b>0.0443</b>	<b>0.0364</b>	<b>0.0589</b>	<b>0.0583</b>
CR		<b>129×</b>	<b>181×</b>	<b>181×</b>	<b>220×</b>	<b>136×</b>	<b>137×</b>

11 sensors across its four fingers. Since human fingers are most sensitive at the distal and proximal ends, each distal and proximal sensor on the dexterous hand is equipped with 120 tactile units, while the intermediate sensors have 60 units each. Hence the hand has a total of 1140 tactile units, each capturing 3-dimensional spatial signals.

#### B. Data collection Method

We construct a multi-point tactile dataset based on PaxiniTech’s multi-degree-of-freedom dexterous hand. The dataset includes four grasping poses: pinch, tripod, cylindrical, and spherical grasping. For each grasping pose, experiments are conducted on eight different objects: apple, egg, orange, tomato, potato, vitamin bottle, water bottle, and glass bottle, as shown in Fig. 2. To enhance data diversity and stability, each combination of object and grasping pose is repeated 10 times for data collection.

Specifically, the object grasping experiments can be divided into two main steps: grasping and releasing.

1) *Grasping*: For each grasping pose, the dexterous hand grasps the object and vertically lifts it by 0.3 meters to ensure stable grasping. The data collection starts 10 seconds before the grasping action to ensure data accuracy, with each tactile unit capturing 3-dimensional force information.

2) *Releasing*: After lifting the object to a designated position, the dexterous hand holds it statically for 15 seconds to record the tactile feedback at rest. Subsequently, the object is released and the data collection ends. This phase mainly captures the tactile changes during the transition from grasping to release, providing a comprehensive data analyse.

### IV. EVALUATION ON COMPRESSION ALGORITHMS

#### A. Data Preprocessing for Efficient Compression

In this paper, we convert tactile signals into RGB image format and leverage existing image compression tools for efficient data compression.

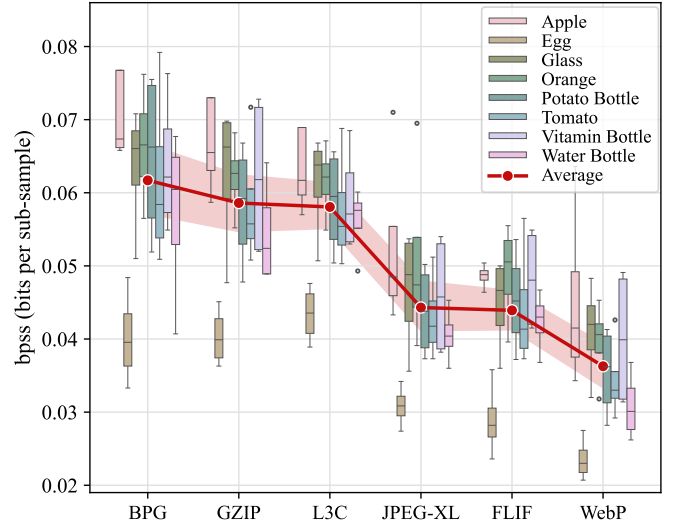


Fig. 4: Lossless compression performance. The x-axis shows various compressors. The y-axis presents their compression efficiency (bps). The boxes indicate performance variation across different grasping poses for each object.

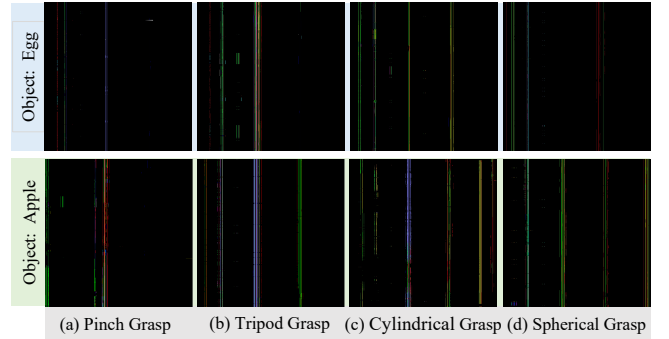


Fig. 5: Visualization of images converted from tactile signals. The first two rows correspond to grasping egg and apple, respectively. The four columns represent four grasping poses.

As illustrated in Fig. 3, the DexH13 dexterous hand integrates 11 sensor arrays, containing 1140 individual sensing units. Each unit captures three-dimensional spatial stress signals relative to its local coordinate system, measuring both parallel and perpendicular components with respect to the local sensor surface. Through real-time fusion of these localized measurements with the hand’s joint angle data, high-resolution contact stress distributions across the entire manipulator can be reconstructed.

After collecting tactile signals for a duration of  $T$ , we concatenate them along the temporal dimension, forming a matrix of size  $(1140, T, 3)$ . These values are then directly mapped to the RGB channels, creating an RGB image with a resolution of  $1140 \times T$ . This approach not only preserves all tactile information but also enables the removal of temporal and sensor redundancies during subsequent data compression process. Furthermore, with such data format conversion, we can also apply computer vision techniques to process tactile signals, such as clustering [34] and classification [35].



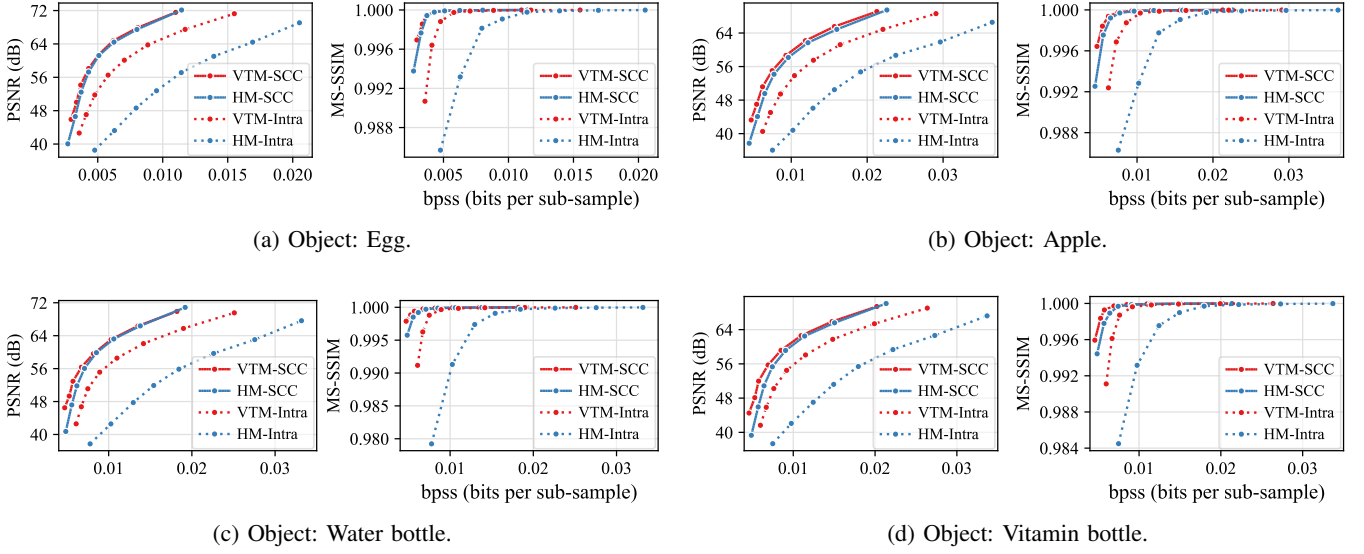


Fig. 6: Lossy compression performance using SCC tools in VTM and HM. Each sub-figure represents grasping an object.

### B. Compression Methods

This paper applies both lossless and lossy compression algorithms to tactile signal images, comparing their compression efficiency to offer a comprehensive evaluation.

Specifically, we employ six lossless compression methods: the neural network-based L3C [12] and five traditional non-neural techniques, namely BPG [36], FLIF [37], JPEG-XL [15], WebP [14], and GZIP [13], to thoroughly assess the compression efficiency of the converted signals. Furthermore, we utilize five classical lossy image codecs to evaluate the rate-distortion (RD) performance of the compressed signals, including the traditional codecs HM (intra mode) [17], VTM (intra mode) [11], JPEG2000 [38], JPEG-XL [15], and the efficient neural-based codec TCM [11]. For those neural-based compression methods (L3C and TCM), we directly use their pre-trained models for compression evaluation.

Besides, as shown in Fig. 3, the tactile images closely resemble screen content, featuring sharp edges, rich high frequencies, and concentrated color distributions. Therefore, we also apply the screen content coding (SCC) [39], [40] tools of HM and VTM for enhanced compression performance.

### C. Lossless Compression Evaluation

Table. I and Fig. 4 illustrate the lossless compression performance of various algorithms for tactile data, measured in bits per sub-sample (bpss). For uncompressed raw data, each sub-sample is stored using 8 bits. The upper part of Table. I summarizes the average performance per algorithm and object, while the bottom part summarizes the average performance per algorithm and grasping pose. In Fig. 4, the x-axis shows compression methods, and the y-axis represents compression efficiency, with lower bpss indicating better performance. The boxes indicate performance variation across different poses (cylindrical, spherical, pinch, tripod) when grasping an object. The red line represents the average performance for each compression method across all objects.

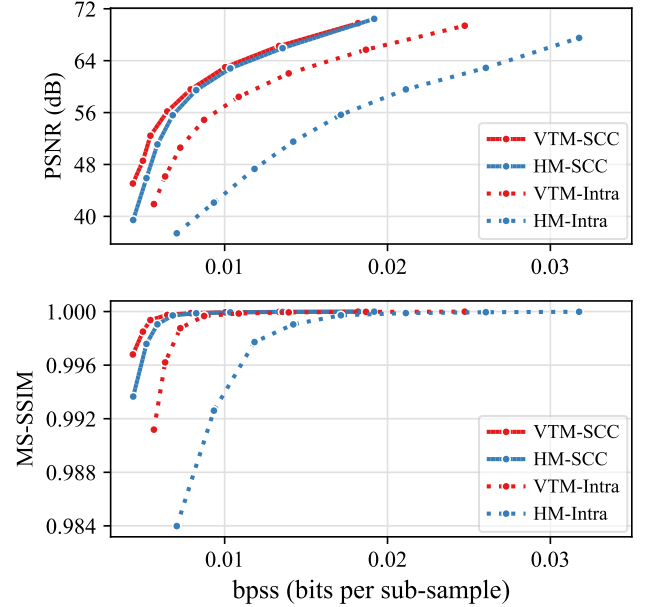


Fig. 7: Average lossy compression performance across all the objects using SCC tools in VTM and HM.

It can be seen from Table. I that all the lossless compressors exhibit satisfactory compression efficiency, with average bpss ranging from 0.0364 to 0.0619, corresponding to compression ratios of 100 to 200 times compared to uncompressed data with bpss of 8.0. While BPG, GZIP, and L3C offer moderate compression performance (0.0583 to 0.0619 bpss), JPEG-XL, FLIF, and WebP achieve notably better results, with average bpss of 0.0441 and 0.0364, respectively. FLIF employs MANIAC entropy coding [37] to dynamically learn data distribution and adapt to various image contents. WebP lossless compression utilizes LZ77 [41] long-match string referencing, making it highly effective for tactile images with repetitive structures.

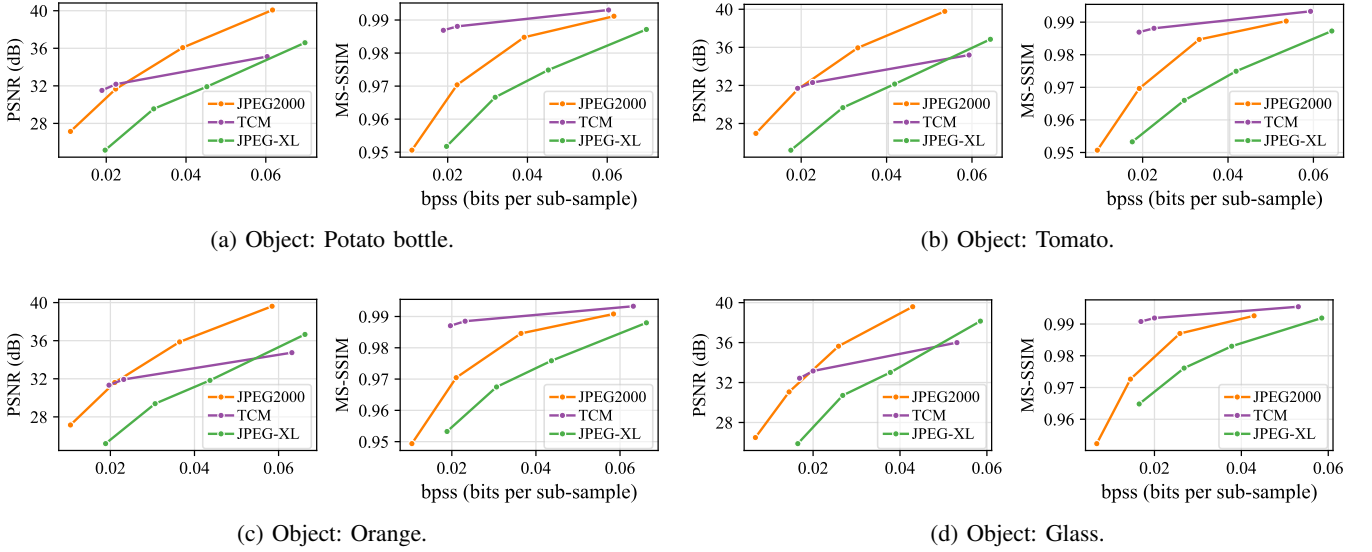


Fig. 8: Lossy compression performance using general-purpose image codecs. Each sub-figure represents grasping an object.

From the lower part of Table. I, it can be observed that the cylindrical grasping presents higher bpss because the tactile is difficult to compress, which implies cylindrical grasping affords greater force pressure. Meanwhile, the precision grasping, including pinch and tripod grasping poses, offers less force. This observation aligns with the typical force distribution in human grasping behavior. Furthermore, across all compressors, tactile signals from grasping eggs achieve the highest compression efficiency, while those from grasping apples and bottles are notably harder to compress. Fig. 5 visualizes the tactile images generated by these two objects under different grasping poses. Eggs are lightweight and geometrically regular, hence produce smoother and more structured tactile images, making compression more efficient. In contrast, apples' irregular shapes and heavier weights introduce more noise and artifacts in the converted tactile images, increasing the compression difficulty.

#### D. Lossy Compression Evaluation

Fig. 6, Fig. 7, Fig. 8, and Fig. 9 illustrate the rate-distortion performance when applying lossy compression, using PSNR [42] and MS-SSIM [43] as the distortion metrics. Given the similarity of the tactile images to screen content, we first apply the state-of-the-art screen content coding (SCC) tools [44] in HM and VTM, comparing their performance against standard intra coding mode, as shown in Fig. 6 and Fig. 7. Notably, HM and VTM maintain reconstruction quality of no less than 38dB at extremely low bit rates ( $<0.01$  bpss, approximately  $800\times$  compression ratios) even using normal intra encoding mode, demonstrating their effectiveness for this task. Similar to lossless compression, lightweight and geometrically regular objects, such as eggs and water bottles, achieve better rate-distortion performance than objects like apples and vitamin bottles, as shown in Fig. 6. Meanwhile, it can be observed that for the same codec, enabling SCC tools largely improves the compression efficiency of tactile

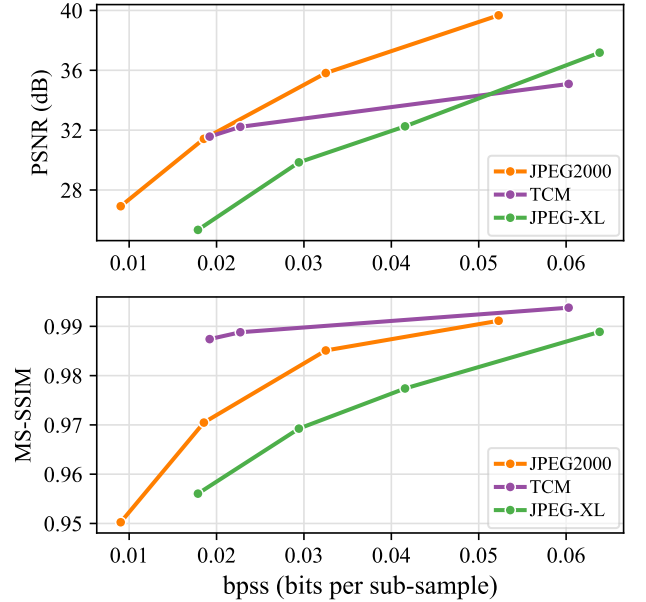


Fig. 9: Average lossy compression performance across all the objects using general-purpose image codecs.

images, achieving 30.67% and 56.42% BD-Rate [45] gains for VTM and HM, respectively.

We also evaluate other lossy image codecs like JPEG2000, JPEG-XL, and TCM, as shown in Fig. 8 and Fig. 9, where the prior demonstrate for distinct objects' compression performance, the latter shows the average performance across all the objects. The three methods are all general-purpose codecs designed for all types of images and deliver moderate compression ratios for our tactile signals. They exhibit inferior encoding performance compared to HM and VTM in both PSNR and MS-SSIM. Neural-based compressors like TCM and L3C often struggle with the generalization capability and perform sub-optimally on such out-of-domain data. However,

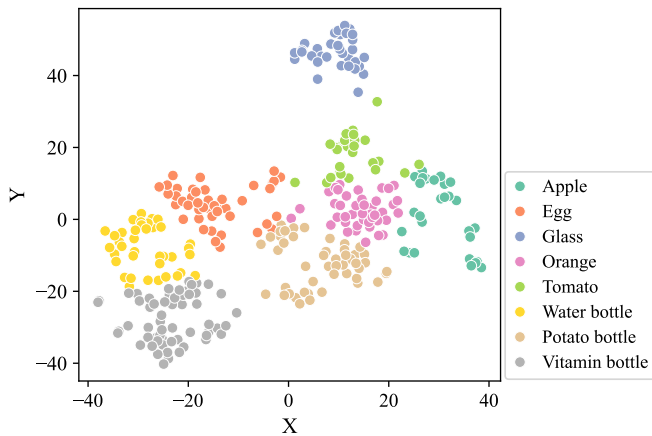


Fig. 10: K-means clustering results on the proposed datasets.

while TCM’s PSNR performance is inferior to JPEG2000, it excels in term of MS-SSIM metric.

#### E. Applications on Downstream Tasks

To validate the effectiveness of the proposed dataset for downstream tasks, we conduct object classification experiments on the generated tactile images. First, we perform a clustering analysis to verify the separability of the generated data. The uncompressed images are projected to 2D space using t-SNE [46], followed by K-means clustering [47] with  $k$  set to the number of object categories. As illustrated in Fig. 10, the tactile images of each object form distinct clusters, indicating that object-specific features are preserved in the dataset and it is feasible to perform object classification.

Then, we simply employ some classical machine learning (ML) methods, including linear regression (LR) [48], support vector machine (SVM) [49], random forest (RF) [50], and K-nearest neighboring (K-NN) [51], to classify the corresponding object of each tactile image. To ensure a balanced evaluation, 70% of the images from each object are randomly selected as the training set, while the remaining serve as the test set. The images are normalized and flattened into vectors as inputs to the classification models. As presented in Table. II, when classifying uncompressed raw images, all these methods achieve at least 70% accuracy, among which SVM and LR perform the best, with accuracies of 81.25% and 79.17%, respectively. LR’s satisfactory performance suggests that tactile image data exhibit relatively well-structured feature distributions. The superior performance of SVM can be attributed to its ability to handle high-dimensional feature spaces and effectively separate complex patterns, making it well-suited for tactile image classification.

Further, we also analyze the impact of compression on object classification using VTM-SCC, the most efficient lossy compressor. As shown in Table. II, compared to performing object classification on raw data, VTM reduces the data volume by a factor of 1200 (i.e., 0.0067 bpss), while still maintaining high classification accuracy (over 70% with SVM and LR). When the data volume is compressed by a factor of 500 (i.e., 0.016 bpss), the resulting distortion has

TABLE II: Object classification accuracy on raw data and VTM-SCC compressed data using different classifiers.

Data	bpss	SVM	RF	K-NN	LR
<b>Raw Data</b>	8.0000	81.25%	76.04%	70.93%	79.17%
<b>VTM-SCC</b>	0.0160	80.21%	72.92%	65.62%	76.04%
	0.0110	77.08%	71.88%	64.58%	73.96%
	0.0067	72.92%	66.67%	61.45%	70.83%

minimal impact on the classification task, particularly for SVM (with only 1% accuracy loss compared to classifying the uncompressed raw data). These results demonstrate the robustness of the proposed dataset for downstream tasks and highlight the effectiveness of our compression methods in reducing tactile data size while retaining essential information for accurate classification.

#### V. CONCLUSION

To achieve high transmission and realtime processing for dexterous manipulation, in this paper we construct a first benchmark of multi-point tactile data compression. First, we introduce the Dex-MPTD, a multi-point tactile dataset for dexterous hand grasping, which captures tactile signals across various sensors, objects, and grasping poses. This dataset serves as a valuable benchmark for advancing research in tactile perception and robotic dexterous manipulation. Second, to address the challenge of high data bandwidth in multi-point tactile sensing, we extensively explore lossless compression techniques by converting tactile signals into images and leveraging modern image compression codecs. Experiments demonstrate that lossless compression can reduce tactile data to 0.0364 bits per sub-sample, achieving up to  $200\times$  compression ratio. Efficient lossy compressors achieve approximately  $1000\times$  data volume reduction while maintaining acceptable fidelity. Further, we investigate general-purpose and SCC-targeted lossy compression methods, revealing that screen content coding tools are effective for tactile data compression. Downstream applications have been discussed to demonstrate that the lossy compression methods only result to 1% accuracy loss for classification task, compared to uncompressed data, which illustrates the efficiency of utilized compression methods. Our codes and dataset will be released upon acceptance.

#### REFERENCES

- [1] Andrew J Bremner and Charles Spence. The development of tactile perception. *Advances in child development and behavior*, 52:227–268, 2017.
- [2] Wenzhen Yuan, Siyuan Dong, and Edward H Adelson. Gelsight: High-resolution robot tactile sensors for estimating geometry and force. *Sensors*, 17(12):2762, 2017.
- [3] Daniël Van Den Berg, Rebecca Glans, Dorian De Koning, Fernando A. Kuipers, Jochem Lugtenburg, Kurian Polachan, Prabhakar T. Venkata, Chandramani Singh, Belma Turkovic, and Bryan Van Wijk. Challenges in haptic communications over the tactile internet. *IEEE Access*, 5:23502–23518, 2017.
- [4] Brayden Hollis, Stacy Patterson, and Jeff Trinkle. Compressed sensing for tactile skins. In *2016 IEEE International Conference on Robotics and Automation (ICRA)*, pages 150–157. IEEE, 2016.

- [5] Yitian Shao, Vincent Hayward, and Yon Visell. Compression of dynamic tactile information in the human hand. *Science advances*, 6(16):eaaz1158, 2020.
- [6] Eckehard Steinbach, Matti Strese, Mohamad Eid, Xun Liu, Amit Bhardwaj, Qian Liu, Mohammad Al-Ja'afreh, Toktam Mahmoodi, Rania Hassen, Abdulmotaleb El Saddik, et al. Haptic codecs for the tactile internet. *Proceedings of the IEEE*, 107(2):447–470, 2018.
- [7] Ariel Slepian, Michael Zakariaie, Trac Tran, and Nitish Thakor. Wavelet transforms significantly sparsify and compress tactile interactions. *Sensors*, 24(13):4243, 2024.
- [8] Hang Lu, Ximeng Tan, Mingkai Chen, Zhe Zhang, Xuguang Zhang, Jianxin Chen, Xin Wei, and Tiesong Zhao. Cross-modal haptic compression inspired by embodied ai for haptic communications. *IEEE Transactions on Multimedia*, 2025.
- [9] Yiwen Xu, Qingfeng Huang, Quanfei Zheng, Ying Fang, and Tiesong Zhao. Perception-based prediction for efficient kinesthetic coding. *IEEE Signal Processing Letters*, 2024.
- [10] Yijing Watkins, Oleksandr Iaroshenko, Mohammad Sayeh, and Garrett Kenyon. Image compression: Sparse coding vs. bottleneck autoencoders. In *2018 IEEE Southwest Symposium on Image Analysis and Interpretation (SSIAI)*, pages 17–20. IEEE, 2018.
- [11] Jinming Liu, Heming Sun, and Jiro Katto. Learned image compression with mixed transformer-cnn architectures. In *Proceedings of the IEEE/CVF conference on computer vision and pattern recognition*, pages 14388–14397, 2023.
- [12] Fabian Mentzer, Eirikur Agustsson, Michael Tschannen, Radu Timofte, and Luc Van Gool. Practical full resolution learned lossless image compression. In *Proceedings of the IEEE/CVF Conference on Computer Vision and Pattern Recognition (CVPR)*, pages 10629–10638, 2019.
- [13] Jean loup Gailly and Mark Adler. Gnu gzip. <https://www.gnu.org/software/gzip/>, 1992. Accessed: 2025-02-28.
- [14] Google. Webp image format. <https://developers.google.com/speed/webp>, 2010. Accessed: 2025-02-28.
- [15] JPEG XL Team. Jpeg xl image coding system. <https://jpeg.org/jpegxl/>, 2021. Accessed: 2025-02-28.
- [16] Joint Video Experts Team (JVET). Vvc test model (vtm). <https://jvet.hhi.fraunhofer.de/>, 2020. Accessed: 2025-02-28.
- [17] Joint Collaborative Team on Video Coding (JCT-VC). Hvc test model (hm). <https://hevc.hhi.fraunhofer.de/>, 2013. Accessed: 2025-02-28.
- [18] Siwei Ma, Xinfeng Zhang, Chuanmin Jia, Zhenghui Zhao, Shiqi Wang, and Shanshe Wang. Image and video compression with neural networks: A review. *IEEE Transactions on Circuits and Systems for Video Technology*, 30(6):1683–1698, 2019.
- [19] K Ahanat, ACR Juan, and P Veronique. Tactile sensing in dexterous robot hands-review. *Rob. Auton. Syst.*, 74:195–220, 2015.
- [20] Tong Li, Yuhang Yan, Chengshun Yu, Jing An, Yifan Wang, Xiaojun Zhu, and Gang Chen. Vtg: A visual-tactile dataset for three-finger grasp. *IEEE Robotics and Automation Letters*, 9(11):10684–10691, 2024.
- [21] Jun Yang, Dong Li, and Steven L Waslander. Probabilistic multi-view fusion of active stereo depth maps for robotic bin-picking. *IEEE Robotics and Automation Letters*, 6(3):4472–4479, 2021.
- [22] Raunaq Bhirangi, Abigail DeFranco, Jacob Adkins, Carmel Majidi, Abhinav Gupta, Tess Hellebrekers, and Vikash Kumar. All the feels: A dexterous hand with large-area tactile sensing. *IEEE Robotics and Automation Letters*, 8(12):8311–8318, 2023.
- [23] Nathan F Lepora. The future lies in a pair of tactile hands. *Science Robotics*, 9(91):eadq1501, 2024.
- [24] Subramanian Sundaram, Petr Kellnhofer, Yunzhu Li, Jun-Yan Zhu, Antonio Torralba, and Wojciech Matusik. Learning the signatures of the human grasp using a scalable tactile glove. *Nature*, 569(7758):698–702, 2019.
- [25] Shubham Kanitkar, Helen Jiang, and Wenzhen Yuan. Poseit: A visual-tactile dataset of holding poses for grasp stability analysis. In *2022 IEEE/RSJ International Conference on Intelligent Robots and Systems (IROS)*, pages 71–78, 2022.
- [26] Jun Yang, Yizhou Gao, Dong Li, and Steven L. Waslander. Robi: A multi-view dataset for reflective objects in robotic bin-picking. In *2021 IEEE/RSJ International Conference on Intelligent Robots and Systems (IROS)*, pages 9788–9795, 2021.
- [27] Kuniyuki Takahashi and Jethro Tan. Deep visuo-tactile learning: Estimation of tactile properties from images. In *2019 International Conference on Robotics and Automation (ICRA)*, pages 8951–8957. IEEE, 2019.
- [28] Javier Cepriá-Bernal and Antonio Pérez-González. Dataset of tactile signatures of the human right hand in twenty-one activities of daily living using a high spatial resolution pressure sensor. *Sensors*, 21(8):2594, 2021.
- [29] Alberto Garcia-Garcia, Sergio Orts-Escolano, Sergiu Oprea, Jose Garcia-Rodriguez, Jorge Azorin-Lopez, Marcelo Saval-Calvo, and Miguel Cazorla. Multi-sensor 3d object dataset for object recognition with full pose estimation. *Neural Computing and Applications*, 28:941–952, 2017.
- [30] Bruno Monteiro Rocha Lima, Venkata Naga Sai Siddhartha Danyamraju, Thiago Eustaquio Alves de Oliveira, and Vinicius Prado da Fonseca. A multimodal tactile dataset for dynamic texture classification. *Data in Brief*, 50:109590, 2023.
- [31] Gyan Tatiya, Jonathan Francis, and Jivko Sinapov. Transferring implicit knowledge of non-visual object properties across heterogeneous robot morphologies. In *2023 IEEE International Conference on Robotics and Automation (ICRA)*, pages 11315–11321. IEEE, 2023.
- [32] Yiming Zhao, Taehun Kwon, Paul Strel, Marc Pollefeys, and Christian Holz. EgoPressure: A dataset for hand pressure and pose estimation in egocentric vision. *arXiv preprint arXiv:2409.02224*, 2024.
- [33] PaXiniTech. Dexh13 dexterous hand. Online, 2024. Accessed: 2025-02-28.
- [34] Glenn Fung. A comprehensive overview of basic clustering algorithms. 2001.
- [35] Dengsheng Lu and Qihao Weng. A survey of image classification methods and techniques for improving classification performance. *International journal of Remote sensing*, 28(5):823–870, 2007.
- [36] Fabrice Bellard. Bpg image format. <https://bellard.org/bpg/>, 2014. Accessed: 2025-02-28.
- [37] Jon Sneyers. Flif - free lossless image format. <https://flif.info/>, 2015. Accessed: 2023-10-01.
- [38] ISO/IEC. Jpeg 2000 image coding system. <https://www.jpeg.org/jpeg2000/>, 2000. Accessed: 2025-02-28.
- [39] Jizheng Xu, Rajan Joshi, and Robert A Cohen. Overview of the emerging hevcc screen content coding extension. *IEEE Transactions on Circuits and Systems for Video Technology*, 26(1):50–62, 2015.
- [40] Tung Nguyen, Xiaozhong Xu, Felix Henry, Ru-Ling Liao, Mohammed Golam Sarwer, Marta Karczewicz, Yung-Hsuan Chao, Jizheng Xu, Shan Liu, Detlev Marpe, et al. Overview of the screen content support in vvc: Applications, coding tools, and performance. *IEEE Transactions on Circuits and Systems for Video Technology*, 31(10):3801–3817, 2021.
- [41] Jacob Ziv and Abraham Lempel. A universal algorithm for sequential data compression. *IEEE Transactions on information theory*, 23(3):337–343, 1977.
- [42] Jari Korhonen and Junyong You. Peak signal-to-noise ratio revisited: Is simple beautiful? In *2012 Fourth international workshop on quality of multimedia experience*, pages 37–38. IEEE, 2012.
- [43] Ilya Bakurov, Marco Buzzelli, Raimondo Schettini, Mauro Castelli, and Leonardo Vanneschi. Structural similarity index (ssim) revisited: A data-driven approach. *Expert Systems with Applications*, 189:116087, 2022.
- [44] Xiaozhong Xu and Shan Liu. Overview of screen content coding in recently developed video coding standards. *IEEE Transactions on Circuits and Systems for Video Technology*, 32(2):839–852, 2021.
- [45] Gisle Bjontegaard. Calculation of average psnr differences between rd-curves. *ITU SG16 Doc. VCEG-M33*, 2001.
- [46] Laurens Van der Maaten and Geoffrey Hinton. Visualizing data using t-sne. *Journal of machine learning research*, 9(11), 2008.
- [47] John A Hartigan and Manchek A Wong. Algorithm as 136: A k-means clustering algorithm. *Journal of the royal statistical society. series c (applied statistics)*, 28(1):100–108, 1979.
- [48] George AF Seber and Alan J Lee. *Linear regression analysis*. John Wiley & Sons, 2012.
- [49] Marti A. Hearst, Susan T Dumais, Edgar Osuna, John Platt, and Bernhard Scholkopf. Support vector machines. *IEEE Intelligent Systems and their applications*, 13(4):18–28, 1998.
- [50] Steven J Rigatti. Random forest. *Journal of Insurance Medicine*, 47(1):31–39, 2017.
- [51] Leif E Peterson. K-nearest neighbor. *Scholarpedia*, 4(2):1883, 2009.